IOP PUBLISHING JOURNAL OF PHYSICS D: APPLIED PHYSICS

J. Phys. D: Appl. Phys. **42** (2009) 115307 (6pp) doi:10.1088/0022-3727/42/11/115307

Determination of correlation length for thickness fluctuations in thin oxide and fluoride films

S E Tyaginov[1,2], M I Vexler[2,3], N S Sokolov[2], S M Suturin[2], A G Banshchikov[2], T Grasser[1] and B Meinerzhagen[3]

[1] Christian Doppler Laboratory and Institut für Mikroelektronik, Technische Universität Wien, Gußhausstr. 25-29, 1040 Vienna, Austria

[2] A F Ioffe Physical-Technical Institute of the Russian Academy of Sciences, Polytekhnicheskaya Str. 26, 194021 St Petersburg, Russia

[3] Institut für Elektronische Bauelemente und Schaltungstechnik, Technische Universität Braunschweig, Hans-Sommer-Str. 66, 38106 Braunschweig, Germany

E-mail: tyaginov@iue.tuwien.ac.at

Received 11 March 2009, in final form 24 April 2009
Published 21 May 2009
Online at stacks.iop.org/JPhysD/42/115307

Abstract

A novel technique for experimental estimation of the correlation length of insulator thickness fluctuations is proposed which is based on the statistical treatment of the results of current measurements for a random set of thin metal–insulator–semiconductor (MIS) capacitors. For testing purposes, the usual Al/SiO_2/Si tunnel diodes with excessive thickness dispersion, as well as the less popular but potentially interesting Au/CaF_2/Si structures, are taken. The verification is performed by a direct comparison of correlation lengths yielded by the new method with those obtained by diagnostics of the same dielectric films using atomic force microscopy.

1. Introduction

One of the critical issues in the field of reliability of thin-film devices is the fluctuation of parameters [1]. Along with the efforts undertaken towards its reductions, a very important task is the determination of values quantitatively characterizing non-homogeneity. This especially concerns the deviations of thickness. Evidently, the smaller its nominal value d_n is, the more significant are any fluctuations. The problems related to the insulator thickness variations in ultra-small field-effect transistors and in metal–insulator–semiconductor (MIS) tunnel devices have been touched upon in the literature of the last decade many times (e.g. [2–6]).

Thickness fluctuation reflects the combination of the metal–insulator and the Si–insulator interface roughness, both of which are processing-regulated. Usually for a local film thickness d, the normal distribution with a standard deviation σ_d is adopted [4–6]. However, spatial fluctuations cannot occur arbitrarily abruptly. To account for this, an additional parameter—correlation length of thickness variation, λ—is introduced which acts as a minimal distance between two points where the local thicknesses are considered independent. Like σ_d, the parameter λ is an overall quality criterion of the insulating film. While the nonzero σ_d causes the shift of all device characteristics from the targeted ones, the finiteness of λ leads to the device-to-device spread, if their linear dimension L is comparable to or less than λ.

The expected dependences of the current spread on the L/λ ratio can be calculated. But here we deal with the inverse procedure of extracting the correlation parameter λ from the data on currents for a selection of MIS diodes. First we more carefully define the 'correlation length' and then explain the proposed technique in detail. Further, we motivate the choice of samples. The next section is devoted to the experimental results, to their treatment yielding the values of λ and to verification. The paper is rounded off by a conclusion.

2. Definition of correlation length

If $d(x)$ is the dependence of thickness on the coordinate in a semiconductor/insulator interface plane, the covariance

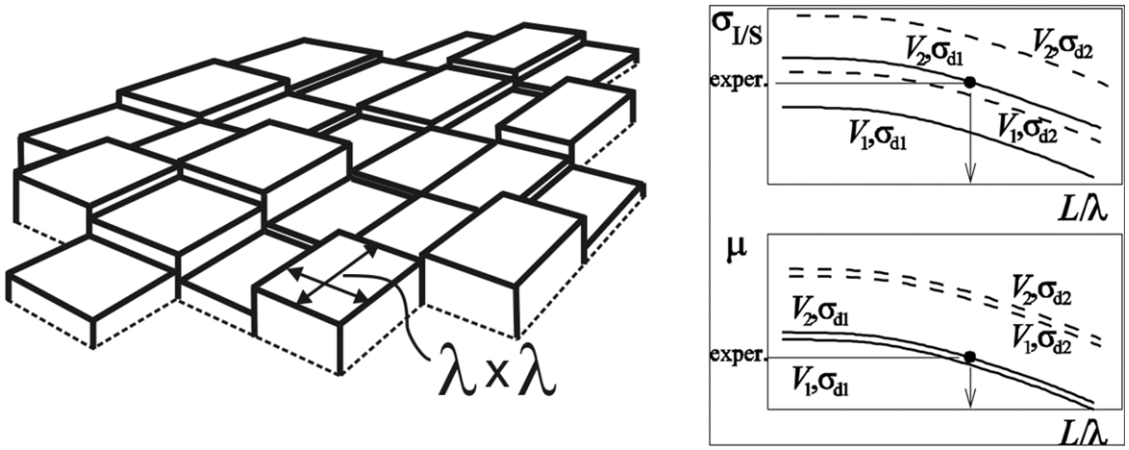

Figure 1. Left: planar fragmentation of the insulator film by the grid with fixed cell size λ. Within each cell, d is assumed to be constant. Right: procedure of the experimental determination of the parameter λ (schematically) using the simulated curves and the experimental value of current dispersion.

between local thicknesses at the distance l is written as

$$\mathrm{cov}(l) = \frac{\langle (d(x) - d_\mathrm{n}) \cdot (d(x+l) - d_\mathrm{n}) \rangle}{\sigma_\mathrm{d}^2}. \qquad (1)$$

In the limit of $l \to 0$, cov tends to 1 due to a full correlation between the thicknesses at two points with infinitesimal distance. Oppositely, if l is very large, $d(x)$ and $d(x + l)$ are independent quantities, and the mean value of the product in (1) evidently equals zero.

Often, the parameter λ is defined as a value of l at which the covariance (1) is reduced to some small value $\mathrm{cov}_\mathrm{crit}$. Alternatively, it may be assumed that cov(l) obeys a Gaussian ($\sim \exp(-l^2/\lambda^2)$) or an exponential ($\sim \exp(-l/\lambda)$) function [2], and, in order to get λ, the measured dependence cov(l) is fitted near $l = 0$ to one of these functions. Of course, these approaches yield different results. Furthermore, cov(l) and λ may exhibit planar anisotropy; if the latter is ignored, angular averaging must be performed in addition.

In fact, there is so far no consensus on some details around the definition of λ, and it would perhaps be more fair to call this parameter the 'characteristic' rather than the 'correlation' length, to avoid any terminological inconsistency.

3. Technique for determination of the correlation length

3.1. Proposed experimental procedure

Our procedure targeting the determination of λ is based on the statistical analysis of a sample-to-sample current spread in a selection of MIS structures.

The analysis is performed within the model reported in [7] presuming the planar fragmentation of the insulator film by a grid with fixed cell size λ (figure 1). Inside each λ × λ cell, the thickness is considered to be constant. The number of involved cells depends on the device area $S = L^2$ through the L/λ ratio. Such a simplification may seem to be a crude approximation of physical reality, but it should be accurate enough taking the uncertainty in the definition of λ into account.

Using this model, the standard deviation $\sigma_{\mathrm{I/S}}$ of the averaged current density I/S at a given bias V can be evaluated. However, a much more universal quantity is the normalized standard deviation $\mu = \sigma_{\mathrm{I/S}}/\langle I/S \rangle = \sigma_\mathrm{I}/\langle I \rangle$. Our extensive simulations showed that μ is much less dependent on the applied voltage V, nominal thickness d_n, substrate doping $N_{\mathrm{A|D}}$, etc, than $\sigma_{\mathrm{I/S}}$. The factor μ and its functional dependence on L/λ are strongly influenced only by the dielectric thickness dispersion. The curve $\mu = \mu(L/\lambda)$ becomes flatter with increasing deviation σ_d.

If measured currents I from a random selection of samples are available, one can calculate σ_I and convert it to $\sigma_{\mathrm{I/S}}$ or to $\sigma_\mathrm{I}/\langle I \rangle$. Using the corresponding simulated curves, the ratio of L/λ can be determined, and consequently λ is known for a given electrode size L (figure 1, $\sigma_\mathrm{d}^{\mathrm{exper.}} = \sigma_{\mathrm{d1}}$ is suggested). It is more convenient to work with μ, as due to the universality of this quantity, the correlation length λ can be reasonably estimated, even if the wafer doping parameters, d_n value or bias conditions in experiment and in simulation are not identical.

The standard deviation of thickness σ_d required for the above procedure can be rather precisely evaluated using the slope of the current–voltage characteristics of large-area MIS structures [7] fabricated on the same wafer.

3.2. Simulation of the current spread factor

The proposed experimental technique evidently relies on the knowledge of the $\mu(L/\lambda)$ dependences for the studied system. So it is necessary to provide the information on how to generate such dependences. A possible algorithm is presented in a flowchart, figure 2.

For each of K_dev devices ($k = 1, 2, \ldots, K_\mathrm{dev}$), first, the number of involved λ × λ cells n_k is defined. If the device borders are assumed to be parallel to the cell grid lines but randomly shifted from them [7], n_k may equal $(\mathrm{E}a + 1)^2$, $(\mathrm{E}a + 1)(\mathrm{E}a + 2)$ or $(\mathrm{E}a + 2)^2$ with probabilities of $(1 - a + \mathrm{E}a)^2$, $2(1 - a + \mathrm{E}a)(a - \mathrm{E}a)$, $(a - \mathrm{E}a)^2$, where $a = L/\lambda$ and $\mathrm{E}a = \mathrm{Entier}(a)$.

For each cell ($i = 1, 2, \ldots, n_k$), the thickness is randomly selected by weighting with a truncated normal distribution G_+;

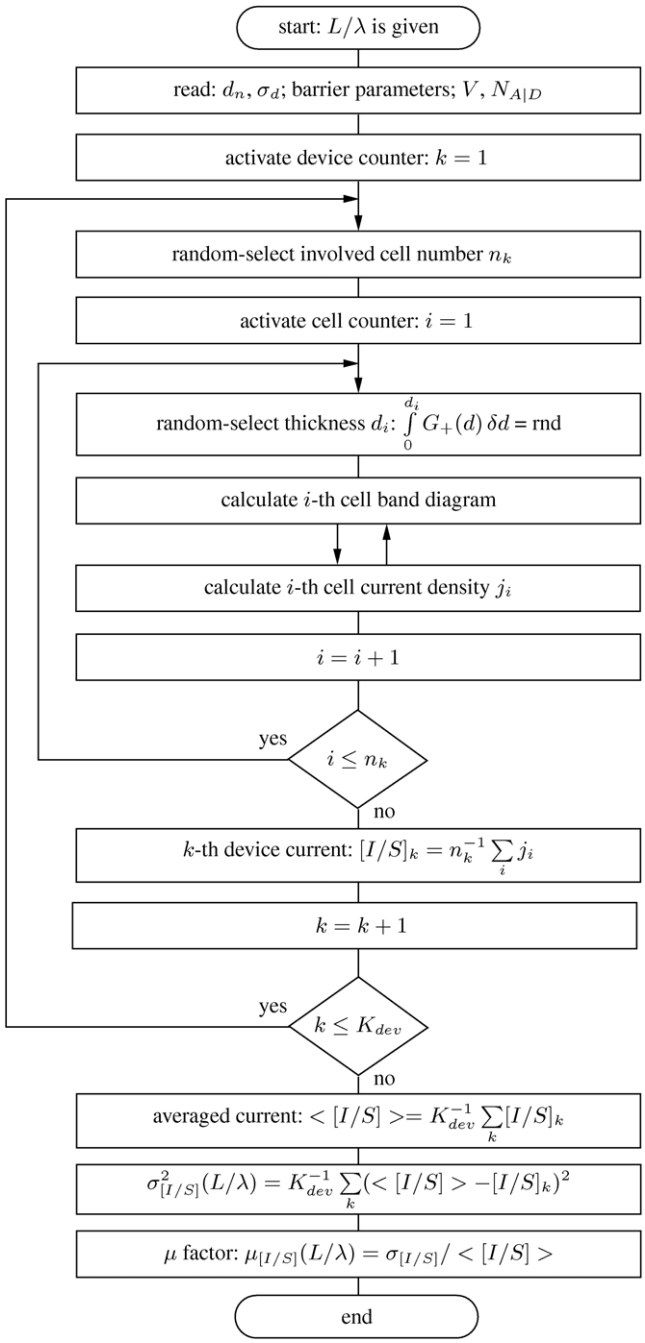

Figure 2. Simulation flowchart for the current spread parameter μ used in the determination of the correlation length.

rnd is a random number between 0 and 1. The band diagram and the current density at a fixed thickness d_i can be calculated using conventional widely published theories of MIS tunnel structures. The arrows in both directions indicate that in some cases, e.g. for the reverse bias conditions, the currents and the voltage partitioning in a structure should be simulated self-consistently. Further details concerning the calculation of j_i for the dielectrics studied in this work will be given at the beginning of section 5.

The averaged current density I/S in the kth device is obtained by the summation of local current densities followed by division of the sum by the cell number n_k. As the factor λ is expected to exceed several nanometres, the transverse quantum effect is negligible [8]. We also ignore the fact that the near-border cells are involved only partly, treating them as fully involved. Afterwards, we average I/S over all the devices, find the current dispersion and calculate the μ factor. The whole routine is to be run with a series of L/λ ratios so as to get a dependence.

This schema admits some optimizations saving computation time, as concretized in [7].

4. Testing structures. Sample fabrication

Our goal is to test the new technique and not the achievable technology level. Therefore, we did not attempt to work with the best possible samples and preferred the ones more suitable for demonstration. This choice is explained below.

4.1. Oxide structures

The first devices used as a test bench are Al/SiO_2/n-Si MIS (i.e. MOS) tunnel structures. We selected them because all tunnelling parameters for this system, such as barrier heights, are well known [9].

These structures were fabricated on n-Si ($N_D \sim 10^{16}$ cm^{-3}) wafers. A thin SiO_2 layer with an averaged thickness $d_n = 2.7$ nm was grown by dry thermal oxidation. The size of a tunnel oxide window was 10×10 or 10×20 μm^2. Large-area devices were also available.

It is worth emphasizing that the examined oxide films had $\sigma_d = 0.28$ nm, which noticeably exceeds the regular values in the modern silicon technologies [1]. However, for this study, a large dispersion of d is advantageous, as it reinforces the effect of thickness variations on the device characteristics. Furthermore, if σ_d is very small, the current spread could be suspected to reflect not the thickness fluctuation but the processing deficiencies of another kind.

4.2. Fluoride structures

For the second test bench, Au/CaF_2/n-Si(1 1 1) structures are selected. They provide an additional verification of the proposed technique, and at the same time they are very promising structures.

Calcium fluoride is a crystalline insulator with a wide (12.1 eV) band-gap and rather high (8.43) permittivity. Due to the small lattice mismatch to silicon, it is considered as a prospective material for silicon-based resonant-tunnelling diodes, superlattices and some other devices [10]. Low leakage makes CaF_2 a prime candidate for gate insulator in field-effect transistors [11].

Thin fluoride films (6–7 monolayers, 3.15 Å each) were grown on the Shiraki-cleaned Si surfaces ($N_D \sim 10^{15}$ cm^{-3}) by the molecular-beam epitaxy. Growth temperature was 250 °C. The process was controlled by high-energy electron diffraction. The gold contacts were $\varnothing = 80$ μm in diameter. In general, the quality of our fluoride layers was good (cf e.g. [10]) and represented the modern level of the CaF_2 on Si technology. Due to the optimization of the growth conditions,

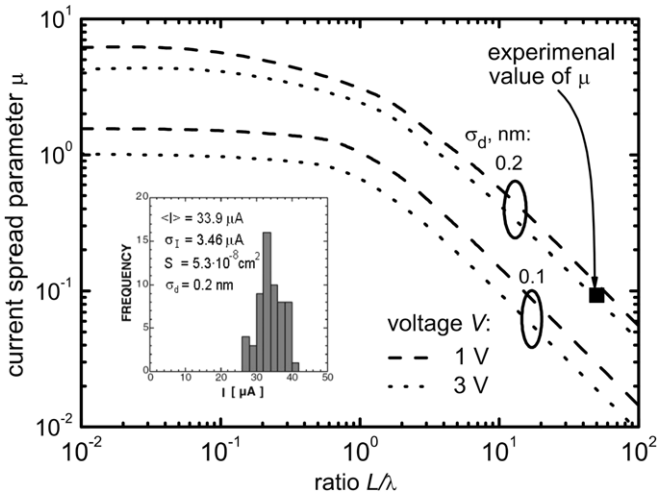

Figure 3. The dependence $\mu = \mu(L/\lambda)$ calculated for Al/SiO_2/n-Si structures with $d_n = 2.5$ nm. The circle marks the parameter of μ from the data on statistical scattering of current in our samples (inset histogram) and the square—the parameters μ from [12].

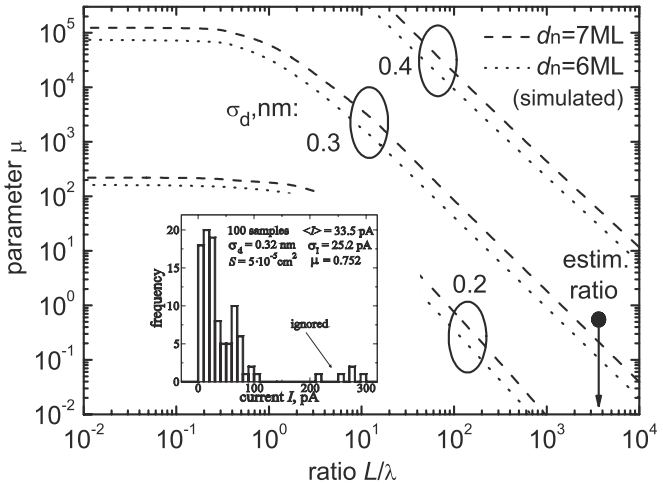

Figure 4. The dependence $\mu = \mu(L/\lambda)$ calculated for Au/CaF_2/n-Si structures at $V = 0.5$ V. 1 ML = 3.15 Å. The filled circle indicates the μ value obtained from the experimental data shown in the histogram.

the formation of triangle pinholes typical for fluoride films was almost suppressed.

The estimated standard deviation of the fluoride film thickness σ_d was 0.32 nm. A comparison with silicon dioxide σ_d values makes no sense, as the materials are quite different.

5. Results and discussion

5.1. Generated current dispersion curves

The simulation of current dispersion relies on the calculation of tunnel characteristics for $\lambda \times \lambda$ cells (section 3). The models for a homogeneous MIS system are known [9], but the difference between the SiO_2 and CaF_2 cases must be mentioned. In the oxide, the carriers from the metal tunnel to the Si conduction band via an 'upper' barrier and to the valence band via a 'lower', while in fluoride, any transport occurs in an 'upper' part of a huge forbidden gap. Moreover, in crystalline CaF_2, the transverse electron momentum is conserved, which must be regarded especially for Si(1 1 1).

Essential simulation parameters are: electron effective mass in SiO_2 ($0.42\,m_0$) and in CaF_2 ($1.0\,m_0$); hole mass in SiO_2 ($0.33\,m_0$); barrier height at the Al/SiO_2 interface (3.17 eV) and at the Au/CaF_2 interface (2.63 eV); SiO_2/Si conduction band offset (3.15 eV) and CaF_2/Si offset (2.38 eV).

The simulated dependences of μ on L/λ for Al/SiO_2/Si capacitors with different standard deviations σ_d (accumulation regime) are presented in figure 3. Equivalent results for CaF_2 devices are shown in figure 4. The curves corresponding to the same σ_d, but to different voltages or different d_n lie close to each other. This confirms the universality of μ pointed out in section 3. The overall role of σ_d is more critical for CaF_2 than for SiO_2, due to the stronger current density dependence on d in the former case because of a larger effective mass.

In the limit of a small L/λ ratio, the parameter μ approaches a finite value of $[\int j^2(d)G_+(d)\delta d / (\int j(d)G_+(d)\delta d)^2 - 1]^{1/2}$ where j is the current density for the thickness d. Near $L/\lambda \sim 1$, the parameter μ begins to decrease, and it falls to zero for large ratios. Note that the vertical axis of figures 3 and 4 is logarithmic. The transition zone becomes broader with increasing σ_d.

5.2. Measurements. Values of correlation length

Computer-controlled current measurements were performed using a Keithley-2400 unit. To avoid damaging the Au/CaF_2/n-Si samples, a connection to gold electrodes was provided by the conductive cantilever of the atomic force microscope (AFM). To feed a current into the Al/SiO_2/n-Si structures, ordinary needles were put onto the deposited contact strips.

The results of our measurements are shown in the insets of figures 3 and 4 as histograms. Among the devices with CaF_2, the spread is more pronounced.

For the Al/SiO_2/Si system (figure 3, area $10 \times 10\,\mu m^2$, i.e. $L \sim 10\,\mu$m) the derived value of μ is about 0.18. From the $\mu = \mu(L/\lambda)$ curves shown in figure 3, we get a L/λ ratio of about 200 and therefore $\lambda \sim 50$ nm. For the structures with twice larger area ($10 \times 20\,\mu m^2$), the factor μ was slightly less, as it qualitatively should be because the correlation length λ does not depend on the device size. From the experimental data published in [12], λ was derived in the same manner as described above. The resulting μ value was 0.102. By coincidence the corresponding correlation length is quite close to our result. Assuming $L = 2.3\,\mu$m (square root from the gate area in [12]) and $\sigma_d \sim 0.2$ nm, we have $L/\lambda \sim 50$ and estimate $\lambda \sim 40$ nm.

For Au/CaF_2/n-Si samples (figure 4, area $\pi \cdot (80\,\mu m)^2/4$, i.e. $L \sim 70\,\mu$m), the resulting parameter μ is 0.75. While calculating it, we ignored several very large current values in the histogram which lie away from the main data pool and arise probably from pinholes. Otherwise we followed the procedure outlined for oxide using the simulated curves of figure 4 and found a L/λ ratio of 3500; this means that $\lambda \sim 20$ nm. To the best of our knowledge, this is the first result reported for

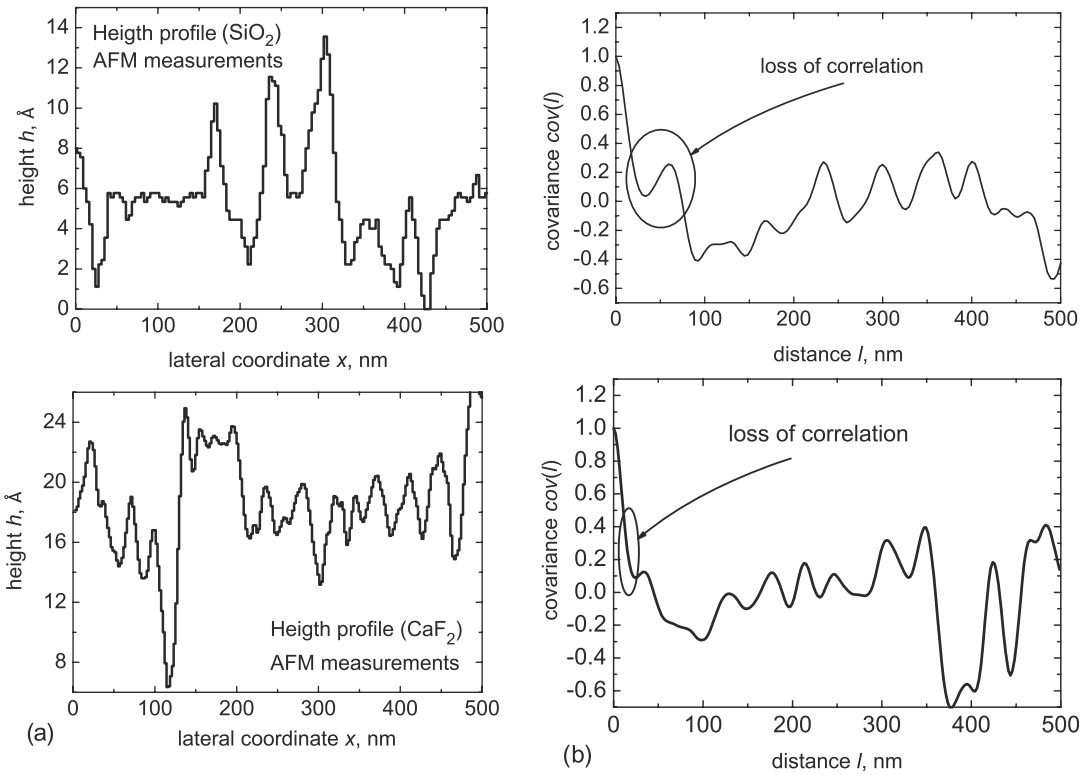

Figure 5. AFM profiles recorded along some direction x in the interface plane (a) and the corresponding covariance functions (b). Upper plots refer to the SiO_2 and lower plots to the CaF_2 films.

thickness fluctuations in CaF_2 layers. Due to a stronger effect of σ_d in the case of fluoride, the obtained correlation length is smaller than in oxide although the measured μ value was larger.

5.3. Verification

For the purpose of verification, we found λ for the same films (outside the deposited electrodes) by the most straightforward way. We simply recorded the height profiles $h(x)$ along some direction using the AFM, and, in order to extract the fluctuation parameter λ, the covariance was calculated assuming $h(x) - \langle h \rangle = d(x) - d_n$ in (1). This assumption is unequivocally correct with respect to the fluoride films as they are formed on the atomically flat wafer, but for the grown oxide the correctness may be questioned. However, since the silicon surface after etching the oxide was rather smooth, we assumed the SiO_2 thickness fluctuations to be completely reflected by the film relief $h(x)$.

The recorded height profiles for SiO_2 and CaF_2 layers are shown in the left plots of figure 5. On the right, corresponding functions cov(l) obtained with equation (1) are shown.

From the data for the oxide, it is easy to derive $\lambda \sim 40$–70 nm. This is in very good agreement with the result of the previous subsection and supports the new method. Some uncertainty is due to the definition of cov_{crit}. No anisotropy in the Si/SiO_2 interface plane has been found. The region $l > 100$ nm within the right plot does not deserve any attention.

In general, the surface relief of the fluoride film is more warped. By interpreting it we got a characteristic length λ of 15–20 nm, again in accordance with the estimate of section 5.1. While working with CaF_2, certain anisotropy was sometimes observed which might be due to the surface steps of the silicon wafer. However, no systematic effect of the miscut angle on the correlation length has been revealed so far, hence it is not possible to claim that the surface steps are just responsible for the value of λ in our fluoride films.

Although the correlation lengths of the thickness fluctuation λ and of the Si interface roughness Λ are different quantities, it is worth noting the following. As discussed in [13], for the post-etching Si surfaces, AFM cannot detect the microrelief on the ~1 nm lateral scale and therefore yields the values of Λ substantially exceeding those deduced from the channel mobility analysis (~1.5 nm). Our method for the determination of λ is also not suitable for this range because the disregarded lateral quantum effects come into play. In principle, such effects may be suggested to mask the thickness variations, which means that the term 'local thickness' and therefore λ have different sense in different situations. This question requires further study, the more so the atomic-scale fluctuations may be important from the point of view of reliability.

6. Conclusion

We have proposed a method of estimating the correlation length λ for the insulator thickness fluctuations in MIS tunnel structures, based on electrical measurements. It implies the statistical treatment of data on current spread in a random set of devices. The knowledge of the parameter λ is important, because λ, together with the standard deviation σ_d, is a quality indicator for a thin insulator film. However, in this work we

neither aimed to use the measurements of correlation lengths for the sample fabrication control nor tried to attain possibly small values of λ. The goal was to demonstrate the new technique.

This technique was successfully examined using two very different types of samples, namely Al/SiO_2/Si diodes with a large (to reinforce all the effects) oxide thickness deviation σ_d, and Au/CaF_2/n-Si(1 1 1) structures with an epitaxial fluoride layer. In both cases, the results from electrical measurements agreed well with the correlation lengths evaluated from direct measurements of the same fluoride or oxide layers using an atomic force microscope.

An advantage of the proposed method is its simplicity because it does not rely on microscopy-aided diagnostics. But there is no proof that the accuracy of our method will be sufficient for very small σ_d, as it can be found in modern CMOS technologies. Therefore, the new method may be potentially more interesting and useful for tunnel-thin films of 'alternative' dielectric materials for which the overall technology level is inferior to that of SiO_2.

Acknowledgments

Acknowledgments This work is supported by the RFBR (Grant 07-02-00900) and FWF (Project 18316-N13). We thank Professor I V Grekhov for useful discussions.

References

[1] International Technology Roadmap for Semiconductors (ITRS)—2008 http://www.itrs.net
[2] Petru A 2004 Analysis of fluctuations in semiconductor devices *PhD Thesis* University of Maryland, USA
[3] Asenov A, Kaya S and Davies J H 2002 *IEEE Trans. Electron Devices* **ED-49** 112–9
[4] Vexler M I, Shulekin A F, Dieker Ch, Zaporojtschenko V, Zimmermann H, Jäger W, Grekhov I V and Seegebrecht P 2001 *Solid-State Electron.* **45** 19–25
[5] Houssa M, Nigam T, Mertens P W and Heyns M M 1999 *Solid-State Electron.* **43** 159–67
[6] Majkusiak B and Strojwas A 1993 *J. Appl. Phys.* **74** 5638–47
[7] Tyaginov S E, Vexler M I, Shulekin A F and Grekhov I V 2005 *Solid-State Electron.* **49** 1192–7
[8] Vexler M I, Grekhov I V and Shulekin A F 2005 *Semiconductors* **39** 1381–6
[9] Schenk A and Heiser G 1997 *J. Appl. Phys.* **81** 7900–8
[10] Watanabe S, Maeda M, Sugisaki T and Tsutsui K 2005 *Japan. J. Appl. Phys.* **44** 2637–41
[11] Sokolov N S, Grekhov I V, Ikeda S, Kaveev A K, Krupin A V, Saiki K, Tsutsui K, Tyaginov S E and Vexler M I 2007 *Microelectron. Eng.* **84** 2247–50
[12] Koh M, Iwamoto K, Mizubayashi W, Murakami H, Ono T, Tsuno M, Mihara T, Shibahara K, Yokoyama S, Miyazaki S, Miura M M and Hirose M 1998 *IEDM Tech. Digest* 919–22
[13] Pirovano A, Lacaita A L, Ghidini G, Tallarida G 2000 *IEEE Electron Devices Lett.* **EDL-21** 34–6